

Exploring Associations between Streetscape Factors and Crime Behaviors Using Google Street View Images

Mingyu Deng¹, Wei Yang()², Chao Chen()^{1,3}, and Chenxi Liu¹

1 School of Computer Science, Chongqing University, Chongqing 400044, China

2 School of Management Science and Real Estate, Chongqing University, Chongqing 400044, China

3 State Key Laboratory of Mechanical Transmission, Chongqing University, Chongqing 400044, China

© Higher Education Press and Springer-Verlag Berlin Heidelberg 2016

Abstract Understanding the influencing mechanism of the urban streetscape on crime is fairly important to crime prevention and urban management. Recently, the development of deep learning technology and big data of street view images, makes it possible to quantitatively explore the relationship between streetscape and crime. This study computed eight streetscape indexes of the street built environment using Google Street View images firstly. Then, the association between the eight indexes and recorded crime events was revealed with a poisson regression model and a geographically weighted poisson regression model. An experiment was conducted in downtown and uptown Manhattan, New York. Global regression results show that the influences of *Motorization Index* on crimes are significant and positive, while the effects of the *Light View Index* and *Green View Index* on crimes depend heavily on the socio-economic factors. From a local perspective, the *Pedestrian Space Index*, *Green View Index*, *Light View Index* and *Motorization Index* have a significant spatial influence on crimes, while the same visual streetscape factors have different effects on different streets due to the combination differences of socio-economic, cultural and streetscape elements. The key streetscape elements of a given street that affect a specific criminal activity can be identified according to the strength of the association. The results provide both theoretical and practical implications for crime theories and crime prevention efforts.

Keywords Crime; Google street view; Streetscape; Spatial analysis; Geographically weighted poisson regression

1 Introduction

It is widely accepted that urban crimes are influenced by the socio-economic, demographic and physical environment of the crime-prone area, and spatially concentrated [1–3]. Recent studies empirically support the role of the built environment in inducing or hindering violent crime [3, 4]. Studies of the “street eye” theory [4], the defensible space theory [5], broken window theory(BWT) [6], crime prevention through environmental design (CPTED) [7], have provided evidence that crime can be prevented through reasonable urban street design and effective use of the built environment [8,9]. Particularly, criminals will determine when, where and what means to commit a crime according to the characteristics of the crime scene. However, due to the lack of precise quantitative data for street scenes, early crime research mainly focused on statistical analysis of the social economy and built environment, ignoring the impact of the streetscape of the visual scene characteristics on crime [10, 11].

Currently, some researches quantify the characteristics of the streetscape by means of remote sensing [12–14], manual audit [2, 15] and questionnaire survey [4]. These existing methods are time-consuming and labor-intensive, and difficult to automatically quantify the characteristics of the street environment from the perspective of human eyes. As a result, the influencing mechanism between streetscape and crime is still unclear, which greatly restricts the application of crime prevention through street design. In the era of big data, big data has broken through the limitation of traditional small-

Received Month dd, yyyy; accepted Month dd, yyyy

E-mail: ywgismap@qq.com; cschaochen@cqu.edu.cn;

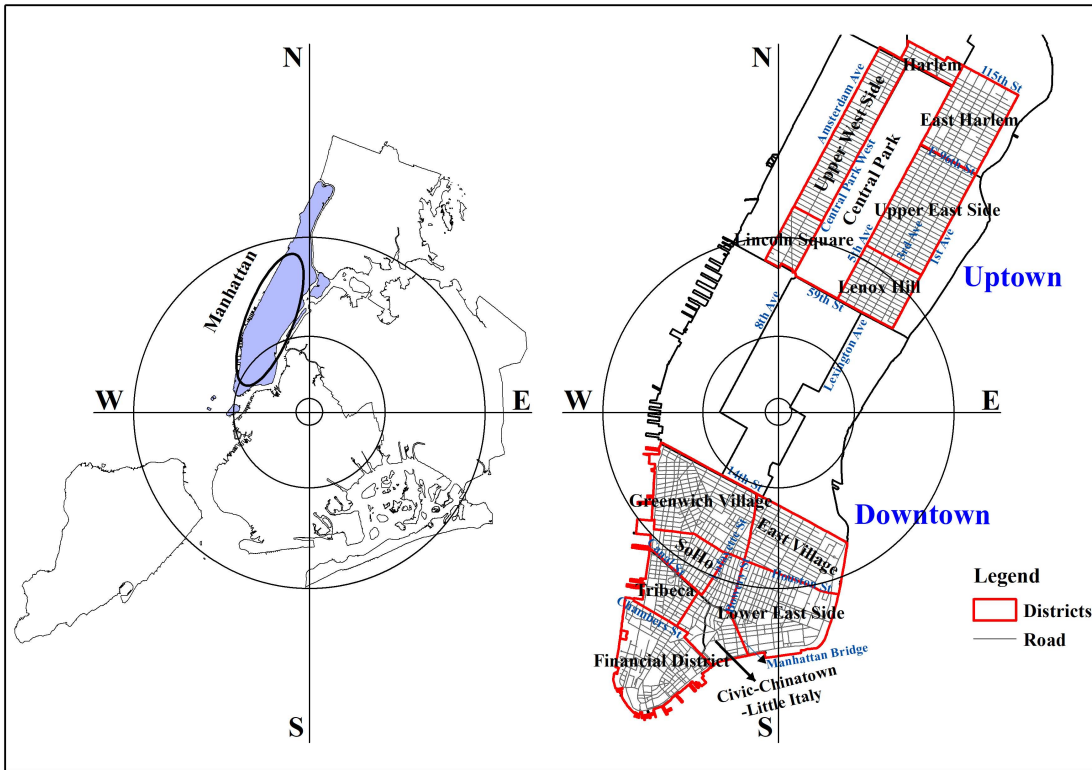


Fig. 1 Study area in Manhattan. The left side of the picture shows the location of Manhattan in New York, and the right side shows the location of downtown and uptown Manhattan.

I data samples. Deep learning technology has become a more powerful tool for image data processing, which makes it possible to study the relationship between streetscapes and criminal activities at street-level [16,17]. Based on the deep learning technology and street view images, quantifying the characteristics of streetscapes and exploring the influence mechanism between streetscapes and crimes, which can make up for the shortcomings of existing researches [2].

Therefore, the following three main hypotheses are tested in this research: 1) What relationship between streetscape factors and criminal events at a global scale? 2) From the perspective of spatial heterogeneity, what relationship between streetscape factors and criminal events at the street segment scale? 3) What are the key streetscape factors that affect criminal activities in specific streets?

2 Data and methods

2.1 Study area and datasets

The study area is uptown and downtown of Manhattan district (as shown in Fig. 1), which is the population, economic and cultural center of New York City. The datasets used in

this study include Open Street Map(OSM) road network data, crime data, Google Street View (GSV) image data, socio-economic data, as shown in Table 1. Crime data is obtained from the New York City Open Data site. The dataset provides a series of spatial and temporal attributes, such as time, date, location, and type of crime incidents. Data from US Census 2010 was used to generate socio-economic and demographic covariates, including population, economy, education, employment, housing, family type, etc. GSV image data is extracted from the GSV website, which is a data service platform where can download a large number of street view images for free.

2.2 Aggregating crime events at street-level

Taking the street segment as the research unit, crime events are aggregated to the nearest street segment with a 50-meter buffer by Geographic Information System after preprocessing the road network. In addition, we divide crime events into violent crimes, property crimes, daytime crimes (6 a.m. to 6 p.m.) and nighttime crimes according to the attribute information of crime incidents. The statistical description of crimes in the study area is shown in Table 2.

Table 1 Datasets of the study area.

Datasets	Description	Data source
Crime data	Including crime location, date, time, etc.	NYC Open Data
Socio-economic data	Demographic, economy, education, housing, family type, etc.	American Factfinder
Map vector data	Road networks, community boundaries, etc.	Open Street Map
GSV image data	Google Street View images.	Google Street View

Table 2 Descriptive statistics for crime events (dependent variables).

Crime variables	Uptown				Downtown			
	Min	Max	Mean	S.D.	Min	Max	Mean	S.D.
Total	0	51	4.58	5.988	0	68	3.88	6.256
Property	0	28	2.30	3.010	0	56	2.36	4.245
Violence	0	43	2.27	4.285	0	31	1.52	3.070
Daytime	0	31	2.44	3.366	0	43	1.62	3.264
Nighttime	0	34	2.13	3.335	0	58	2.27	3.783

2.3 Streetscape variables

2.3.1 GSV images collection and feature extraction

Street view image sampling points are generated along the road network at 100m intervals, and then the street view images are collected according to the coordinates of each sampling point through the Google Street View static API(see Google Maps Platform, accessed December 2019). The GSV panorama of each sampling point is composed of 18 images in six horizontal directions (0° , 60° , 120° , 180° , 240° , 300°) and three vertical angles (-45°, 0°, 45°), as shown in Fig. 2. Finally, 25362 and 37422 images were collected in uptown and downtown respectively after removing pictures of indoor or abnormal through visual inspection.

The DeepLab V3+ [18] deep learning framework was adopted for semantic segmentation and extracting visual physical features from GSV images. Eleven categories of physical elements, including roadways, sidewalks, sky, buildings, trees, grass, vehicles, persons, traffic signs, street lights, and fences were extracted from GSV images, as shown in Fig. 3. Finally, the physical elements extracted from all sampling points of each road segment are aggregated, and the visual elements are quantitatively measured at the street segment scale.

2.3.2 Streetscape indexes calculation

Based on the existing researches and related theories of criminology [9, 12, 13, 19], this paper proposed 8 crime-related indicators using the information extracted from street view images. The calculation formula for each indicator and the reasons for its selection are explained as follows.

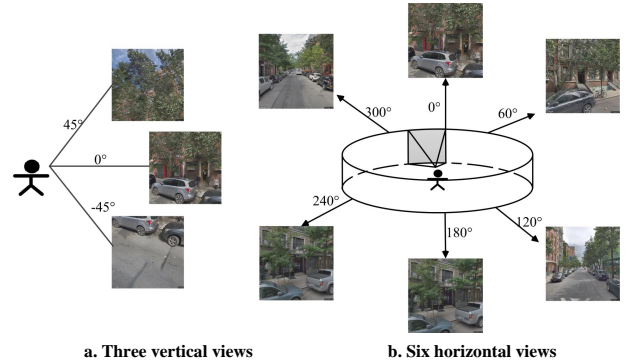


Fig. 2 GSV panoramas captured in six horizontal directions(b.) and three vertical view angles (a.) at a sample site.

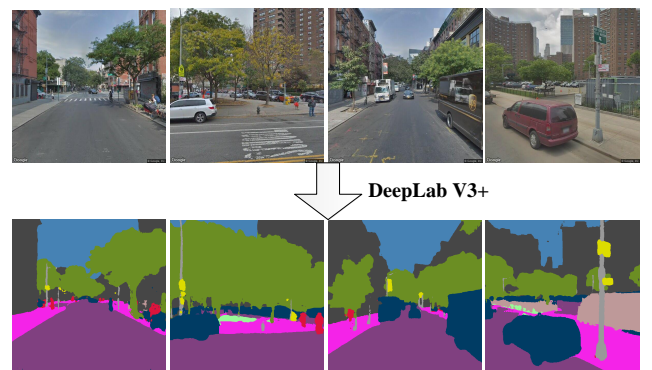


Fig. 3 Semantic segmentation results for the GSV images with the DeepLabV3+ model.

1) *Green View Index (GVI), Building View Index (BVI), Sky View Index (SVI), Light View Index (LVI)*. Existing researchers have proved that using geographic information data can well explore the relationship between environmental indexes(including the richness of vegetation, the attributes of buildings, and street lights, etc.)and criminal activities [9, 12, 13]. Therefore, these indexes are recalculated with street view data in this paper. Referring to the GVI calculation formula proposed by Li et al. [20, 21], the calculation formulas of BVI, SVI, and LVI are proposed respectively. Each indicator is defined as the percentage of pixels associated with the specific elements (i.e. vegetation, buildings, sky, and light) to the total number of pixels in the 18 street view images (i.e. a panorama). For example, the GVI represents the percentage of vegetation pixels to the total number of pixels in a panorama. Therefore, the general calculation formula is defined as follows:

$$VI_{object} = \frac{\sum_{i=1}^6 \sum_{j=1}^3 Pixel_{object}}{\sum_{i=1}^6 \sum_{j=1}^3 Pixel_{total}} \times 100\% \quad (1)$$

object ∈ {greenery, building, sky, light}

where VI_{object} is the percentage of visual elements *object* in a panorama, $Pixel_{object}$ refers to the number of object pixels in one of these images captured in six horizontal directions with three vertical view angles for each panorama, and $Pixel_{total}$ is the total pixel number of 18 GSV images. The variables $VI_{greenery}$, $VI_{building}$, VI_{sky} , and VI_{light} are referred to as GVI, BVI, SVI and LVI for easy understanding, respectively. The higher the GVI value is, the more vegetation there is. In addition, it is known that the properties of building, such as the height, appearance and continuity of the building, have an impact on the occurrence of crime. The BVI reflects the height and continuity of the buildings on both sides of the street in this work. SVI represents the area of sky elements from the

perspective of human eyes, and the larger the SVI value is, indicating that the street vision is more open. The LVI stands for the distribution of street lights.

2) *Pedestrian Space Index (PSI)*. When people are in a crowded street pedestrian space, they are crowded and disorderly, and it is easy to produce uncomfortable experiences (breathing anxiety, irritability, restlessness, etc.). Under such circumstances, the chances of crime are greatly increased (such as thieves). We measure pedestrian crowded space by the ratio of the total pixels of the sidewalk to the total pixels of the roadway in the 18 street view images, namely PSI, which is mostly used to describe the crowded degree of pedestrian walking space. The PSI calculation formula is defined as following equation:

$$PSI = \frac{\sum_{i=1}^6 \sum_{j=1}^3 Pixel_{sidewalk}}{\sum_{i=1}^6 \sum_{j=1}^3 Pixel_{roadway}} \times 100\% \quad (2)$$

where $Pixel_{sidewalk}$ and $Pixel_{roadway}$ respectively refer to the number of total pixels of the sidewalk and roadway in the panoramic image.

3) *Street Canyon Enclosure (SCE)*. Street canyon enclosure is an important factor in people's perception of the environment. In this paper, SCE is used to describe the degree to which visual elements on both sides of a street enclose the street. Streets with greater enclosure usually have a narrow field of view, and therefore lack of more human eye supervision [4], which may breed more criminal activities. Referring to the literature [22, 23], it is defined as the percentage of the total pixels of buildings, trees, traffic signs, and fences to the total number of pixels in the 18 street view images. The SCE calculation formula is defined as Eq.(3).where $Pixel_{building}$, $Pixel_{tree}$, $Pixel_{trafficsign}$, and $Pixel_{fence}$ respectively refer to the number of total pixels of buildings, trees, traffic signs and fences in the panoramic image.

$$SCE = \frac{\sum_{i=1}^6 \sum_{j=1}^3 (Pixel_{building} + Pixel_{tree} + Pixel_{trafficsign} + Pixel_{fence})}{\sum_{i=1}^6 \sum_{j=1}^3 Pixel_{total}} \times 100\% \quad (3)$$

$$MI = \frac{\sum_{i=1}^6 \sum_{j=1}^3 (Pixel_{roadway} + Pixel_{sidewalk} + Pixel_{vehicle})}{\sum_{i=1}^6 \sum_{j=1}^3 Pixel_{total}} \times 100\% \quad (4)$$

$$NAI = \frac{\sum_{i=1}^6 \sum_{j=1}^3 (Pixel_{sky} + Pixel_{tree} + Pixel_{grass})}{\sum_{i=1}^6 \sum_{j=1}^3 (Pixel_{roadway} + Pixel_{sidewalk} + Pixel_{building} + Pixel_{trafficsign} + Pixel_{light} + Pixel_{fence})} \times 100\% \quad (5)$$

4) *Motorization Index (MI)*. The characteristics of road traffic and the nature of roads are also important factors affecting criminal activities [24]. According to empirical literature [22, 23] and common sense, it is defined as the percent-

age of the total pixels of the three types of elements of the roadways, sidewalks, and vehicles to the total pixels in the 18 street view images. The MI calculation formula is defined as Eq.(4), where $Pixel_{roadway}$, $Pixel_{sidewalk}$, and $Pixel_{vehicle}$ re-

Table 3 Descriptive statistics for nine covariates.

Covariates	Uptown				Downtown			
	Min	Max	Mean	S.D.	Min	Max	Mean	S.D.
Population density (people per acre)	34.39	461.66	175.51	71.19	12.05	463.93	115.58	58.65
Vulnerable population(%)	10.92	55.76	34.53	9.39	3.26	45.84	22.67	9.60
Media income(k\$)	1.25	25.00	10.43	5.79	1.11	25.00	10.33	5.84
Poverty(%)	0.00	57.62	12.88	11.25	0.00	78.91	13.93	12.38
Low education(%)	0.00	42.53	5.30	7.42	0.00	65.60	8.93	13.75
Unemployment(%)	0.00	37.10	7.99	5.75	0.00	39.30	6.76	5.01
Female alone(%)	11.07	44.95	27.98	6.38	7.17	38.98	23.14	6.69
Single-parent family(%)	0.29	26.16	5.15	5.56	0.13	20.28	2.54	2.37
Housing vacancy(%)	0.00	47.71	12.46	8.60	0.30	64.85	9.77	8.49

spectively refer to the number of total pixels of roadways, sidewalks, and vehicles in the panoramic image.

5) *Nature Artificial Index (NAI)*. Crime is influenced by the natural and artificial elements of streets. What is the impact of the combination ratio of natural elements and artificial elements on criminal activities? The NAI is proposed to answer this problem. NAI is defined as the percentage of the total pixels of natural elements to the total pixels of artificial elements in the 18 street view images. The NAI calculation formula is defined as Eq.(5), where $Pixel_{sky}$, $Pixel_{tree}$, and $Pixel_{grass}$ respectively refer to the numbers of total pixels of natural elements of the sky, tree, and grass in the panorama. $Pixel_{roadway}$, $Pixel_{sidewalk}$, $Pixel_{building}$, $Pixel_{trafficsign}$, $Pixel_{light}$, and $Pixel_{fence}$ respectively refer to the number of total pixels of artificial elements of roadways, sidewalks, buildings, traffic signs, lights and fences in a panorama. According to the above equations, eight indexes of all sampling points in the street are calculated, and then the weighted average method is adopted to aggregate indexes in the street segment.

2.3.3 Covariates

In this study, we controlled for a series of demographic and socio-economic variables, including population density, percentage of vulnerable population (i.e. the population age under 18 and over 65), median household income, poverty rate, unemployment rate, housing vacancy rate, percentage of the population with low education level (i.e. population with a degree below high school), percentage of females living alone, and percentage of female single-parent households. Table 3 provides descriptive statistics for nine covariates. To be consistent with the analysis unit of street physical factors, the basic unit of 50m buffer of the street is used to calculate nine covariates by weighted average aggregation.

2.4 Global and local regression models

2.4.1 Poisson regression

The global regression is conducted by the Poisson regression model considering that crime events are non-negative discrete values and the crime data distribution conforms to Poisson distribution. The generalized linear Poisson regression formula is defined as follows:

$$\log(\lambda_i) = \beta_0 + \sum_{k=1}^m \beta_k x_{ik} + \varepsilon \quad (6)$$

where, β_0 is a constant, λ_i is the i th road segment expected numbers of crimes (i.e dependent variables), x_{ik} is the k th independent variables for the i th observation, β_k is the corresponding estimated coefficient, and ε is an error term.

2.4.2 Geographically weighted poisson regression

Nonstationarity is another common phenomenon in geographic distribution [25]. However, the Poisson regression model neglects the spatial impacts of variables, and it cannot reveal the spatial dynamics of the relationship between spatial variables. While the geographically weighted regression (GWR) model can solve this problem [26]. Therefore, we combine the GWR and poisson regression as the geographically weighted poisson regression (GWPR) model to investigate the spatial nonstationarity and to investigate the influences on crime activities. GWPR takes the location (u, v) into account, is expressed as follows [26, 27]:

$$\log(\lambda_i) = \beta_0(u_i, v_i) + \sum_{k=1}^m \beta_k(u_i, v_i)x_{ik} + \varepsilon_i \quad (7)$$

where (u_i, v_i) stands for the coordinates of the i th regression 'points', $\beta_0(u_i, v_i)$ is a constant, $\beta_k(u_i, v_i)x_{ik}$ is the coefficient of the k th independent variables x_{ik} at location (u_i, v_i) and ε_i is the i th error term.

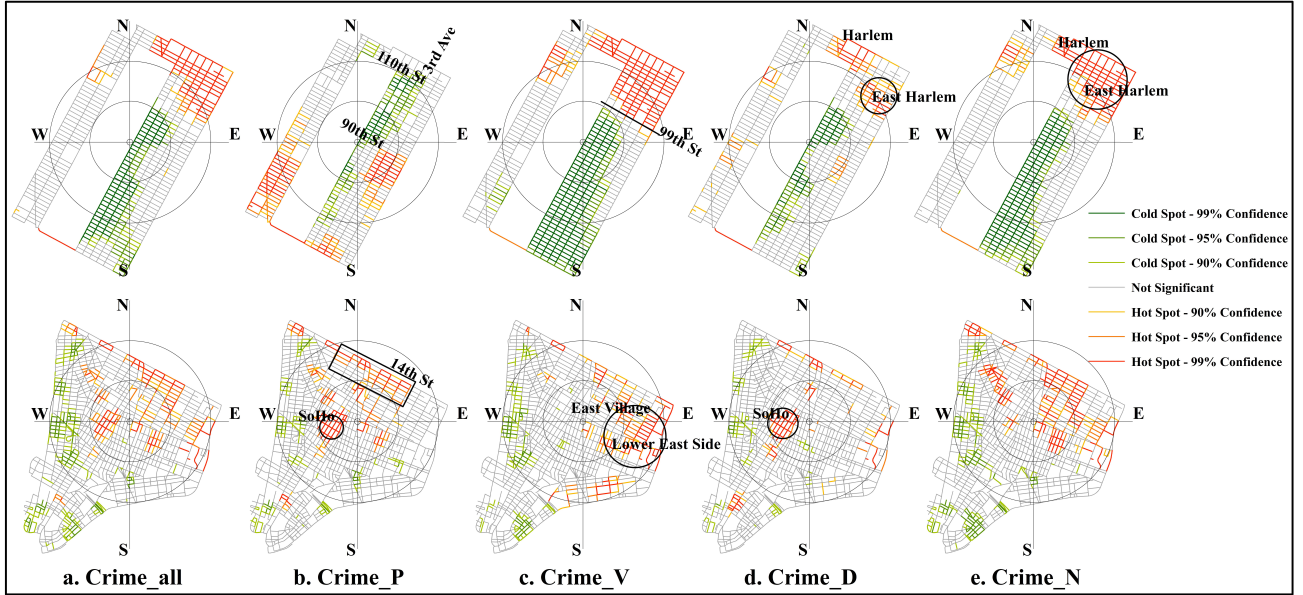


Fig. 4 The results of the Getis-Ord-Gi* for different crime types (a, b, c, d, e).

GWPR can be viewed as a local regression model where the weights associated pairs of geographic data. In the bandwidth selection, the adaptive method considers the density of the samples [26,27]. Therefore, a bi-square adaptive function was used to estimate the weights, and the corrected Akaike Information Criteria (AICc) method was used to automatically adjust the bandwidth in this study [27].

of the hot spots and cold spots of crime also changed over time, as shown in Fig. 4d and Fig. 4e. Hot spots of daytime crime in uptown are concentrated in the middle streets of Harlem and East Harlem; the hot spots of nighttime crime are concentrated in the Harlem and East Harlem district. In downtown, daytime property crimes (such as theft) are most prominent in the south of the SoHo district. The hotspots of crime such as burglary and assault at night are clustered in part of downtown streets.

3 Results analysis

3.1 Spatio-temporal analysis of crimes

The hot spots and cold spots of crime events were analyzed to study the spatial cluster pattern by the Getis-ord Gi* [28] method, as shown in Fig. 4. The distribution of hot spots and cold spots of criminal activities in uptown is more concentrated, while downtown is more dispersed. In uptown, the hot spots of violent crimes (robbery, assault, etc.) are concentrated on the north of 99th street; while the cold spots of property crimes are mostly gathered on the Third Avenue from East 90th Street to East 110th Street, and the violent crimes of cold spots concentrated in the streets below East 96th Street. In downtown, the hot spots of property crimes are concentrated in the south of SoHo district, the northwest of East Village and surrounding the 14th Street of Greenwich Village district. While the hot spots of violent crimes (robbery and assault) are most aggregated in the central and eastern of East Village and Lower East Side. Additionally, the spatial distribution

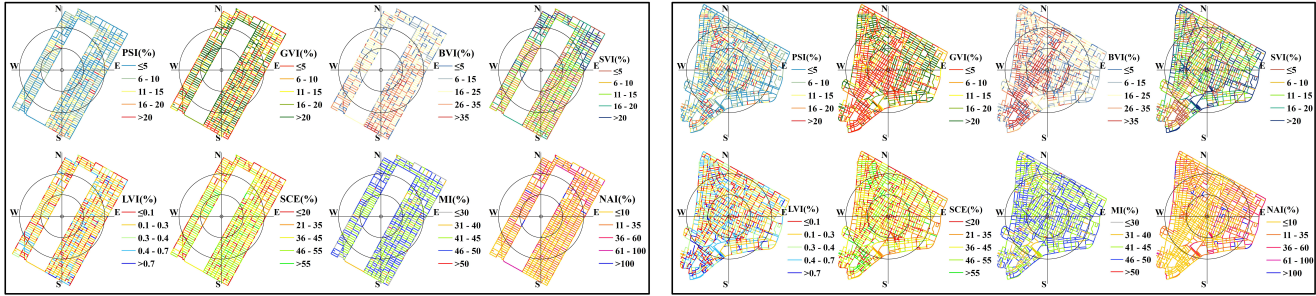
3.2 Analysis of street element indexes

Taking the street segment as the basic unit, eight streetscape indexes are calculated after obtaining the physical elements of GSV, and the overall statistical results are shown in Table 4. As we can see, the LVI value of uptown and downtown is the smallest and the NAI value is the largest. Moreover, the differences between indexes reflect the characteristics of the street visual environment. For example, the mean value of GVI in uptown is much higher than in downtown, which indicates that uptown with a higher greening degree.

The results of eight streetscape indexes are visualized, as shown in Fig. 5. Overall, the average values of the streetscape index in the study is similar, but the average values of GVI and NAI in uptown and downtown are quite different. Compared with downtown, the GVI of uptown is higher because of Central Park accounts for one-third of uptown. On the contrary, the GVI of downtown shows a trend of increasing from southwest to northeast. Meanwhile, it can be seen from

Table 4 Descriptive statistics for eight streetscape indexes (independent variables).

Visual factors(%)	Uptown				Downtown			
	Min	Max	Mean	S.D.	Min	Max	Mean	S.D.
PSI	0.00	33.32	5.54	5.01	0.00	59.02	8.21	7.58
GVI	0.00	78.43	13.47	10.95	0.00	61.54	9.16	10.45
BVI	0.00	57.37	19.23	11.45	0.00	68.68	22.25	15.07
SVI	0.00	36.99	10.95	7.97	0.00	42.93	11.63	8.76
LVI	0.00	1.70	0.23	0.19	0.00	3.14	0.33	0.28
SCE	0.00	81.12	33.79	16.92	0.00	78.19	33.04	18.03
MI	0.00	63.12	37.56	17.20	0.00	64.55	35.64	17.51
NAI	0.00	321.63	17.29	25.26	0.00	6066.70	22.09	165.28



(a) Streetscape factors quantification results in uptown.

(b) Streetscape factors quantification results in downtown

Fig. 5 Visualization results of eight streetscape factors in uptown(a) and downtown(b).

Fig. 5 that the index difference is large in the local area, which is mainly determined by the visual scene characteristics. For instance, there are more streets with higher LVI values in downtown than in uptown, and are concentrated near the streets of the Financial District and SoHo district, as shown in Fig. 5(b). Therefore, the results of streetscape visual indexes quantification are consistent with the actual streetscape, which indicates that the reasonability and validity of the streetscape indexes measurement method.

3.3 Regression results and analysis

3.3.1 Results of the global regression models

The poisson regression models (Models 1-10) were used to explore the global relationship between criminal activities and streetscape factors. The results are reported in Table 5. For different types of crimes (property crimes and violent crimes), MI has the strongest positive correlation with these two types of crimes(Model 2, 3, 5, 6), which indicates that the areas with high mixing degree and accessible road network not only fail to play the role of "street eye" in natural monitoring, but also create opportunities for criminals to commit crimes and escape. This finding agrees with previous studies [4]. However, PSI is negatively correlated with these

two types of crimes (Model 2, 3, 5, 6), which is explained by the fact that crime increase significantly in the streets with narrow pedestrian space (such as alleys, narrow sidewalks) or with wide pavement (easy escape) [24]. The remaining indexes have different effects on different types of crime in different regions. For example, LVI and SCE have the strongest positive correlation with all types of crime in uptown, while this situation is opposite in downtown. Similarly, GVI has a stronger negative correlation with all types of crime in uptown, but this case is opposite in downtown. These opposite results are partly due to differences in regional street environmental characteristics. For example, Central Park occupies a large area of uptown, and many people are resting, socializing, exercising around the park, which increases extensive crowd surveillance and suppresses criminal activities. This is consistent with the regression results. BVI, SVI and NAI have different effects on different crimes. Part of the regression results are the same as the previous studies [2, 17, 29], but the other part is opposite or can not be explained. The reason may be that the effect of visual indexes on crime is non-stationary in space.

For the crimes in different times in Table 5 (Model 7, 8, 9, 10), MI is positively correlated with crimes. The results are similar to the previous study once again [4], and shows a

Table 5 Poisson regression results for different types and times of crimes.

variables	Uptown					Downtown				
	Model 1 (All crime)	Model 2 (Property)	Model 3 (Violence)	Model 7 (Daytime)	Model 8 (Nighttime)	Model 4 (All crime)	Model 5 (Property)	Model 6 (Violence)	Model 9 (Daytime)	Model 10 (Nighttime)
Visual fators										
PSI	-.042**	-.019	-.086**	-.054***	-.027	-.044***	-.047**	-.041	-.124***	.020
GVI	-.166	-.214	-.136	-.352**	.065	.132*	.026	.262**	.235**	.045
BVI	.076	.105	-.015	-.089	.279	.338***	.289**	.303*	.585***	.123
SVI	.021	.007	.044	.031	.014	.055**	-.007	.167***	-.100**	.183***
LVI	.085***	.089***	.080***	.128***	.028	-.224***	-.257***	-.165***	-.202***	-.238***
SCE	.246	.355	.216	.510	-.084	-.245**	-.168	-.276	-.511***	-.015
MI	.464***	.482***	.454***	.398***	.544***	.517***	.650***	.315***	.666***	.387***
NAI	.119***	.118***	.108***	.127***	.107***	-.042**	.008	-.160***	-.050	-.040*
Covariates										
Population density	.137***	.135***	.141***	.087***	.194***	.200***	.196***	.246***	.112***	.270***
Vulnerable	-.162***	-.099***	-.244***	-.066**	-.298***	-.161***	-.046**	-.302***	-.043*	-.267***
Media income	-.031	.068*	-.286***	-.070*	.001	-.155***	-.219***	-.112**	-.227***	-.088**
Poverty	.224***	.169***	.220***	.115***	.325***	.012	.002	.005	.013	.009
Below high	.134***	.170***	.123***	.088**	.184***	-.174***	-.382***	.079*	-.209***	-.131***
Unemployment	-.060***	-.010	-.087***	-.053**	-.063**	.028**	.035*	.039*	.032	.026
Housing vacant	.173***	.146***	.188***	.142***	.199***	-.004	-.007	-.017	.050**	-.093***
Female alone	.116***	.180***	-.020	.124**	.104***	.078***	.005	.147***	-.001	.151***
Female single	.253***	-.085*	.356***	.199***	.315***	.205***	-.059**	.369***	.157***	.243***
Constant										
Intercept	1.249***	.557***	.327***	.68***	.371***	1.173***	.648***	.145***	.408***	.510***
AICc	3988.4	2355.4	2887.8	2882.6	2329.4	9672.7	6557.6	4960.9	5492.3	6142.7
Adjust R ²	0.33	0.27	0.42	0.211	0.372	0.184	0.181	0.24	0.141	0.200

* significant at the 0.1 level, ** significant at the 0.05 level, *** significant at the 0.01 level.

universal law that the MI can promote crime to some extent. Nevertheless, the regression results of LVI and NAI are opposite in uptown and downtown. This is similar to the regression results of LVI and SCE in Table 5 (Model 2, 3, 5, 6), and there is a common reason for differences in regional environmental characteristics. There are also discrepancies in the relationship between the remaining visual indicators and the crimes in different periods. It can be explained by the geographical position and the socio-economic differences [12, 30]. For example, the uptown has apparent advantages in public facilities, street safety, economic, culture, and housing planning, etc., which reduced crime. On the contrary, in downtown, there are obvious disadvantages in socio-economic (such as low income, high poverty, low education, high unemployment, etc.), culture, public security, which increased crime rate to some extent [12].

In summary, MI has a positive correlation with criminal activities and PSI has a negative correlation with crimes through the global regression analysis. However, the regression results of the remaining indexes are opposite or contrary to common sense in different regions. The reason is the effect of visual indexes on crime is non-stationary in space due to the regression results are affected by regional characteristics. Therefore, the necessity of local regression analysis is emphasized.

3.3.2 Results of the GWPR models

Compared with the poisson regression model, GWPR is suitable for dealing with spatial autocorrelation and non-stationary problems, and can further discloses the spatial dynamics of the impact on criminal activities. Table 6 reports the estimated coefficients of the streetscape factors and the fitting degree by the GWPR models. The adjusted R^2 of all GWPR models increased by 20% in comparison with poisson regression models. Meanwhile, the AICc values in all GWPR models are lower than those of the above poisson regression models. These outcomes verify the better explanatory power of the GWPR models.

For the streetscape indexes of single visual elements (including GVI, BVI, SVI, and LVI), Fig. 6 further displays the spatial distribution of the GWPR regression results. Overall, the influence of the four visual indexes is quite different in different streets. The negative correlation between GVI and property crime and violent crime is the strongest on the central streets of the east of uptown, as shown in Fig. 6(a). In downtown, GVI has the strongest positive influence on the property and violent crimes on the streets of Manhattan Bridge, Washington Square Park, and Stonewall Inn. Compared with the environmental characteristics of the two places, the uptown has better city virescence. However, the GVI of the streets with lower socioeconomic will encour-

Table 6 GWPR results for different types and times of crimes.

variables	Uptown(Model 1, 2, 3, 7, 8)						Downtown(Model 4, 5, 6, 9, 10)					
	Min	Max	Mean	S.D.	AICc	Adjusted R ²	Min	Max	Mean	S.D.	AICc	Adjusted R ²
Model 1: (all crime)					2805.2	0.684	Model 4: (all crime)				6721.7	0.471
PSI	-0.1363	0.1288	-0.0013	0.0412			-0.0496	0.0253	-0.0075	0.0178		
GVI	-0.5189	0.3927	-0.0579	0.1508			-0.1674	0.411	0.0287	0.0993		
BVI	-0.5231	0.3317	-0.0361	0.1328			-0.1636	0.4214	0.033	0.1024		
SVI	-0.1927	0.2266	-0.0045	0.0617			-0.0762	0.0996	0.0012	0.0275		
LVI	-2.3134	3.1007	0.1034	0.9398			-1.8426	0.8817	-0.6014	0.5034		
SCE	-0.378	0.459	0.0525	0.1347			-0.4359	0.1782	-0.0232	0.1011		
MI	-0.0553	0.3624	0.0468	0.0467			-0.0049	0.086	0.0327	0.0183		
NAI	-0.0459	0.0834	0.0072	0.0216			-0.0711	0.0171	-0.0078	0.0155		
Model 2: (property)					1963.1	0.537	Model 5: (property)				4873.5	0.445
PSI	-0.0599	0.0596	0.002	0.0258			-0.0514	0.0245	-0.0095	0.0177		
GVI	-0.3488	0.3185	-0.0329	0.1472			-0.1812	0.3566	0.0292	0.0999		
BVI	-0.3232	0.2819	-0.0131	0.1265			-0.1526	0.3933	0.0397	0.1063		
SVI	-0.108	0.1258	-0.0095	0.0405			-0.0827	0.0801	-0.0035	0.0302		
LVI	-1.3349	1.8515	0.2983	0.6152			-1.905	0.161	-0.6806	0.4561		
SCE	-0.2959	0.351	0.0274	0.1383			-0.3807	0.1917	-0.0267	0.102		
MI	-0.0176	0.1425	0.0478	0.0286			-0.0015	0.0779	0.0402	0.0183		
NAI	-0.0176	0.0463	0.0037	0.0139			-0.0897	0.0246	-0.0073	0.0186		
Model 3: (violence)					2294	0.685	Model 6: (violence)				3846.2	0.47
PSI	-0.1409	0.1321	-0.0035	0.0482			-0.0541	0.0447	-0.0035	0.0208		
GVI	-0.5222	0.8727	-0.0074	0.1943			-0.1503	0.3608	0.0251	0.0921		
BVI	-0.4231	0.8665	0.0235	0.1894			-0.1828	0.3427	0.0212	0.0906		
SVI	-0.2745	1.1034	0.0276	0.155			-0.047	0.104	0.0179	0.0278		
LVI	-3.4847	2.8345	0.2415	0.9886			-1.9004	0.9853	-0.5153	0.5348		
SCE	-0.7001	0.8923	0.0333	0.1734			-0.383	0.1649	-0.0143	0.0924		
MI	-0.0567	1.1143	0.0814	0.1635			-0.0382	0.1091	0.0185	0.0247		
NAI	-0.1283	0.1285	0.0059	0.0347			-0.0803	0.0479	-0.009	0.0171		
Model 7:(daytime)					2286.5	0.563	Model 9:(daytime)				4173.8	0.418
PSI	-0.1347	0.0988	-0.0063	0.0359			-0.0608	0.0281	-0.0155	0.0203		
GVI	-0.4559	0.3755	-0.0806	0.1553			-0.2375	0.462	0.0384	0.1113		
BVI	-0.4314	0.3325	-0.0678	0.1389			-0.2055	0.4727	0.0449	0.1163		
SVI	-0.1739	0.2196	-0.0058	0.0546			-0.0955	0.1264	-0.0057	0.0372		
LVI	-2.4273	2.9505	0.4603	0.8929			-2.1237	0.6904	-0.6154	0.525		
SCE	-0.3144	0.3969	0.075	0.1419			-0.4946	0.1913	-0.0365	0.1142		
MI	-0.0443	0.2945	0.0446	0.043			-0.0072	0.0906	0.0398	0.0215		
NAI	-0.0405	0.084	0.0044	0.0209			-0.0644	0.0284	-0.0066	0.0165		
Model 8:(nighttime)					1992	0.564	Model 10:(nighttime)				4509	0.464
PSI	-0.0712	0.0674	-0.0001	0.0302			-0.045	0.0345	-0.0018	0.0186		
GVI	-0.3796	0.2688	-0.0226	0.1348			-0.1933	0.3304	0.0288	0.0948		
BVI	-0.282	0.3134	0.0107	0.1273			-0.1725	0.3392	0.0287	0.0961		
SVI	-0.1117	0.0543	-0.0099	0.033			-0.0445	0.0891	0.006	0.024		
LVI	-2.3105	1.1658	-0.0249	0.5636			-2.0569	0.8576	-0.5614	0.4995		
SCE	-0.2805	0.3503	0.0145	0.1302			-0.3447	0.1997	-0.0191	0.094		
MI	-0.0035	0.1505	0.0445	0.0269			-0.0121	0.0791	0.029	0.0183		
NAI	-0.0196	0.0555	0.007	0.0159			-0.1036	0.0168	-0.0116	0.0202		

age crime, which is the same as the conclusion of the study in [12]. Therefore, with regard to the scale of the street, more attention should be paid to the impact of social economy on crime.

The space distribution of the influence of BVI and SVI on urban crimes are shown in Fig. 6(b)(c). In uptown, BVI has the strongest positive correlation with property crime and violent crime respectively on East Harlem street and the central and northeast of Lenox Hill. These streets are mostly eth-

nic communities (such as Latin) or residential areas, which make the property and violent crimes more frequent. BVI has strong positive effects on property crime and violent crime on the streets around Manhattan Bridge and Washington Square Park of downtown. The reasons are that it is influenced by the social economies, such as CBD, dense POI distribution and mixed population.

Although the effect of the streetscape index is the same in different streets, its explanation mechanism is different due

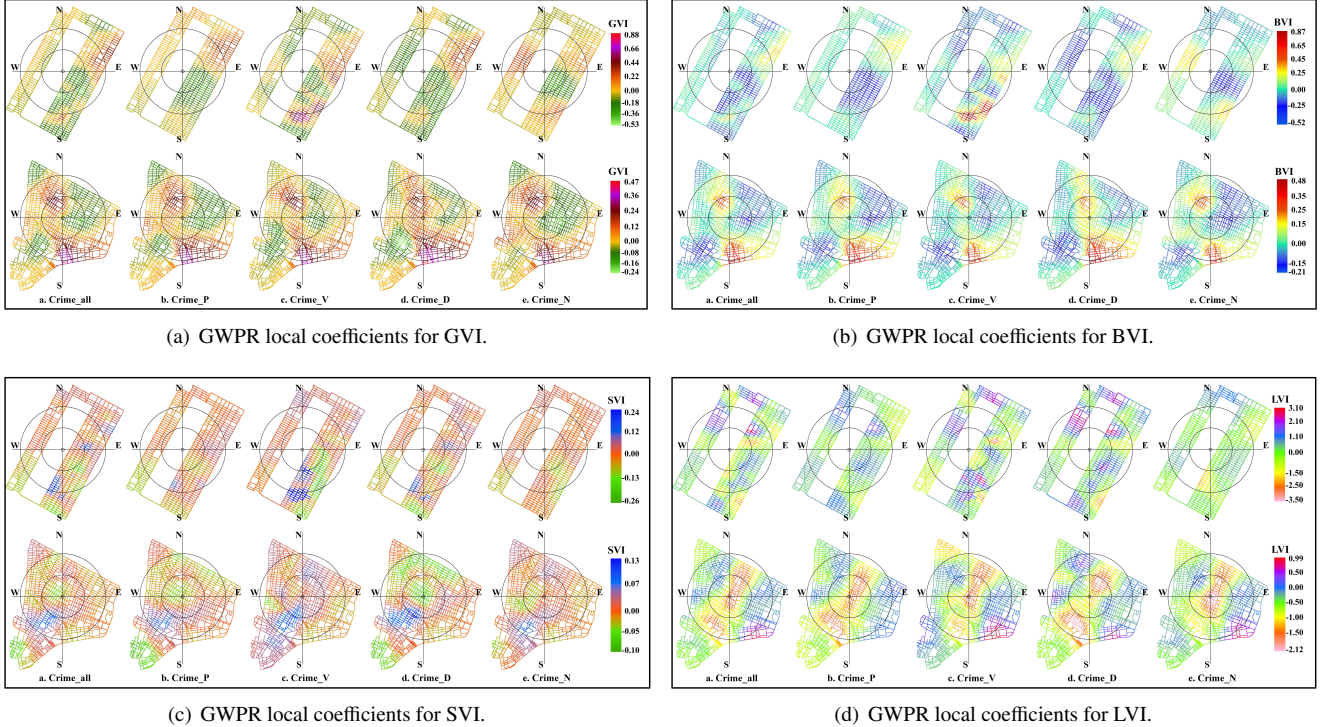


Fig. 6 GWPR local coefficients for GVI, BVI, SVI and LVI.

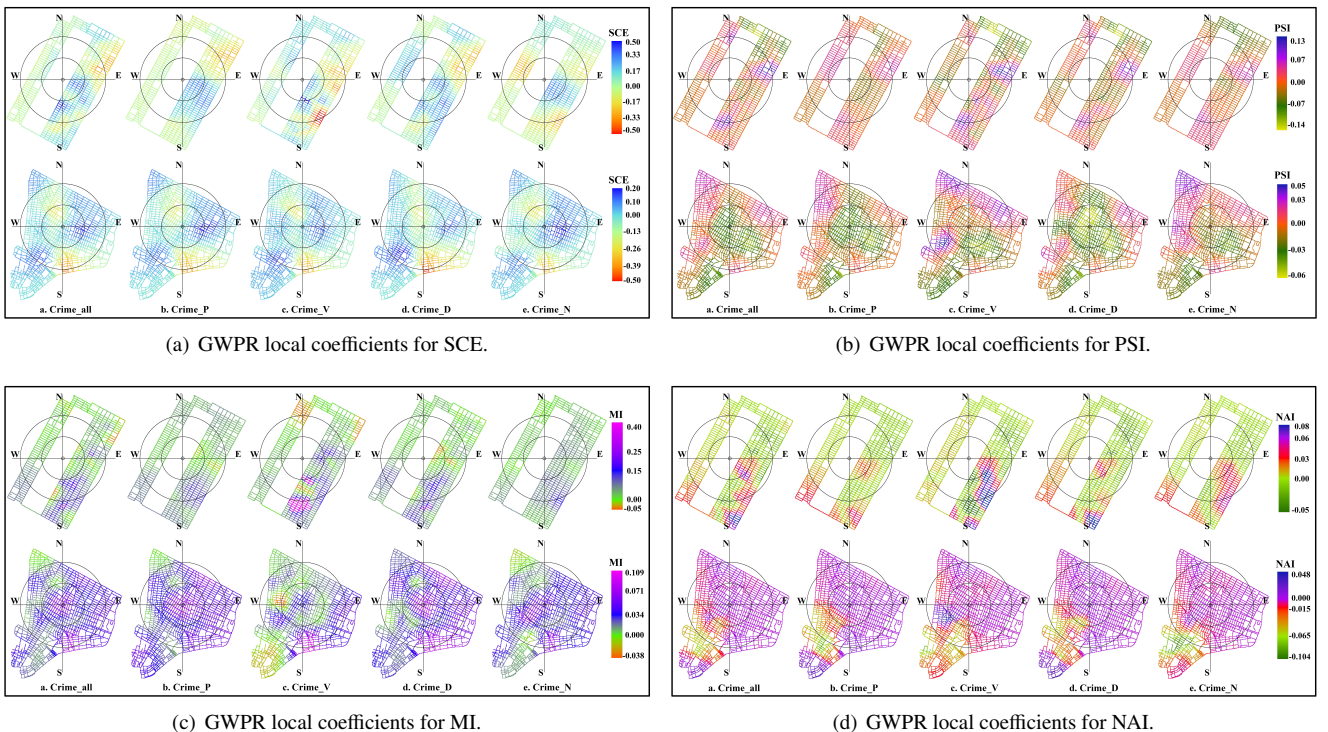


Fig. 7 GWPR local coefficients for SCE, PSI, MI and NAI.

to the complexity of the environment. The influence of SVI on criminal activities is implicit as shown in Fig. 6(c). No matter from global regression (Table 5) results or local regression results, its influence is not obvious. For the impact of LVI on crime, there are significant spatial differences, as shown in Fig. 6(d). The streets (such as central and northeast of Lenox Hill, Lincoln Square, SoHo, Financial District, and Bowery street, etc.) with dense population and POI, obvious social and economic advantages, the bigger the LVI is, the stronger the inhibition of night crime and property crime is. This finding is consistent with the research conclusion in literature [9] and the common sense that more street lights will strengthen eye surveillance. On the other hand, increasing lighting on the streets (such as the streets of the Lower East Side and Washington Square Park) with obvious economic disadvantages promotes the occurrence of crime. The reason is that socio-economic factors play a decisive role in the crime on these streets.

For the streetscape indexes of the combinations of visual factors (including SCE, PSI, MI, and NAI), the spatial distribution of the GWPR regression results is visualized in Fig. 7. Fig. 7(a) shows that the rate of property crimes such as theft has increased on the streets with higher SCE. The main reason is that the street canyon area is crowded and secretive, which is convenient for theft. In contrast, the rate of violent crimes such as physical assault and robbery is reduced on the streets with higher SCE. The narrow roads and crowded people in the street canyon area are not convenient for criminals with obvious criminal behaviors to escape. In Fig. 7(b), the spatial distribution difference of the PSI coefficients indicates that the influence of the socioeconomic and physical environment of different streets on criminal activities is different. For instance, with the increase of PSI, violent crimes have increased significantly on the streets with obvious socioeconomic disadvantages (e.g., streets in Harlem and Lower East Side) and dense POIs (e.g., northwest Greenwich Village, northeast East Village, etc.), as shown in Fig. 7(b). The spatial differences are the result of the social-economic factors and streetscape factors. The influence of the MI on criminal activities and its spatial distribution is shown in Fig. 7(c). The MI of all streets in the study areas is positively correlated with property crime and violent crime. Especially, for the downtown streets of SoHo, East Village, Lower East Side, and Chinatown, the POI diversity, population density, traffic busy degree and other factors jointly promote the occurrence of criminal events with MI. From global regression (Table 5) results to local regression results, MI has a strong positive correlation with criminal activities, and this finding

is consistent with existing literature [4]. The spatial distribution of the impact of NAI on criminal activities is shown in Fig. 7(d), which indicates that the regularity of its influence is not strong, and the spatial difference of its influence is small. According to the GWPR regression results, we can get the correlation intensity of different types of crime affected by different streetscape indexes in each street segment. Based on the correlation, we can find out the key factors that affect different criminal activities for each street segment. For example, compared with the remaining 7 indicators, LVI has the strongest inhibitory effect on nighttime crimes on Bowery Street (Fig. 6(d)). Therefore, it can be considered that LVI is a key factor affecting nighttime crimes for Bowery Street.

Based on the above analysis, the following important findings are drawn: 1) The spatial influence of NAI and SVI on crime is relatively gentle. 2) The influence intensity of PSI, GVI, LVI, BVI, and MI on criminal activities has significant changes in space, and LVI changes most dramatically. B-VI has strong positive effects on property crime and violent crime. LVI has stronger inhibition of nighttime crimes and property crimes. 3) The influence of streetscape on criminal activities and its spatial heterogeneity will be affected by specific geographical location and socio-economic factors. This means that the same streetscape factor may have different effects on different crimes in different places. 4) Based on the GWPR results, it can find out the key visual streetscape elements that affect the occurrence of specific criminal activities for each street.

3.4 Discussion

This paper combines GSV and deep learning technology to automatically quantify the characteristics of streetscape firstly. Then the impact relationship of eight streetscape indexes on different types of criminal activities and its spatial heterogeneity were explored by the poisson regression models and GWPR models. Although the findings contribute to crime prevention through urban design, the following aspects still need to be further discussed:

- 1) In this paper, the regression model is used to explore the influence of streetscape factors on criminal activities and the spatial differences of the influence from a global and local perspective. On the one hand, the relationship between streetscape factors and criminal activities is mostly complex and nonlinear. On the other hand, various streetscape factors, socioeconomic factors, individual attributes, and personal perception of the street environment are intertwined with each other, which jointly affect the occurrence of criminal be-

havior. Therefore, it is still necessary to further explore the impact of different combinations of streetscape elements and individual subjective perception of the street environment on criminal activities.

2) The influence of streetscape factors on crime is also affected by socioeconomic, and the difference is significant. For example, for the streets with high socioeconomic, perfect public facilities and security police forces (such as the central and eastern streets of the Upper East Side,), the influence of the social economy on crime is much stronger than that of LVI. Therefore, despite more street lights are added, the crime rate will not be greatly affected. Consequently, in some specific streets, the influences of socioeconomic factors on crime may far exceed the streetscape factors, or the streetscape factors even can be ignored.

3) Compared with poisson regression models, GWPR is more suitable to explore the difference and nonstationary of the impact of streetscape elements on criminal activities. And the key streetscape elements that affect criminal activities can be identified at the street-level from the local analysis results based on the GWPR model. For example, we can find out the key streetscape elements affecting specific criminal activities in each street according to the GWPR results from Fig. 6 to Fig. 7. This can provide decision-making suggestions for urban street design.

4) This study provides a practical case for exploring the influence mechanism of the streetscape and criminal activities, and the relevant conclusions are consistent with some of the existing results. The conclusion in this study can be used to prevent crime through street design, but the influence of socioeconomic factors can not be ignored.

al attributes and population by taking account of the diversity among cities and using a regression analysis, which indicated the role of cities' economic deprivation, high population density, deterrents, poverty, and inequality as causes of crime [1–3, 29, 32, 33]. Meanwhile, the impact of environments such as POIs [34, 35], road network [24, 36], land use, public infrastructure [37] and street environment [2, 37, 38] on criminal activities have been paid more and more attention, and it has been gradually applied to urban crime intervention in urban planning, street design, and other fields with the further development of BWT and CPTED theory. For example, the crime rate inference problem was studied by utilizing large-scale POI data and taxi flow data in the city of Chicago, USA [34]. The impact of road network and tree coverage on different criminal activities was investigated at street scale respectively [38, 39], and the results showed that road accessibility, tree coverage, and road density were associated with burglary and property crime. The relationship between street crime and physical characteristics of the street was studied by the logistic regression model and geographically weighted regression(GWR) model [10, 33]. However, the above researches mostly used conventional methods such as remote sensing, questionnaire, and manual audit to obtain built environment data, which was costly, time-consuming and difficult to automatically and quantitatively measure the street environment from the perspective of visual scenes. Limited by the means of data acquisition, it is still unclear about the influencing mechanism between the streetscape factors and urban crime.

4.2 Streetscape factors and crime

The primary criminological theories underlying current empirical studies of environmental correlates of crime are B-WT and CPTED [2, 15]. CPTED argued that crime and fear of crime can be inhibited through proper design and modification of physical features of the residential environment. Therefore, various studies have explored the relationship between crime and street built environment [2, 15]. For example, the crime (such as robbery, burglary, etc.) occurrence mechanism was analyzed by integrating the built environment data (such as POI data, remote sensing data), socioeconomic factors, individual attributes and other factors at the neighborhood scale [12–14]. However, the built environment data is obtained by the remote sensing and mapping technique, which can not quantify the vertical dimension of street environment characteristics (such as the vertical surface of high buildings, street canyon, etc.) due to the top

4 Literature review

4.1 Factors in crime occurrence

Existing studies in criminology had tried to demonstrate the relationship between crime and various influencing factors [2, 29, 31–33]. These factors can be generally categorized into social-economic and urban environment factors. Socio-economic factors mainly include economy [29, 31, 32], social culture (race, religion, education, etc.), demographic [2, 33] and unemployment [29]. Early studies considered the relationships between inequality, unemployment rate and crime for urban counties and demonstrated that income inequality and high unemployment rate have higher crime rates. Recent researches gradually studied socio-economic, individu-

view of remote sensing instead of the real horizontal view of pedestrians. This makes the deep influence mechanism of the real scene perception and the driving force of the streetscape scene elements on the criminal behavior cannot be explored completely.

Recently, with the development of big data and intelligent technology, crowdsourced data like geo-tagged pictures, trajectory data [40–44], street view images have become an important means for urban sensing and social sensing [45, 46]. Especially, deep learning technique [47] is widely used to quantitatively obtain street physical features such as vegetation, buildings, roads, sky, and vehicles from street view images (e.g. Google, Baidu, Tencent, etc.) [20, 21, 48]. Compared with conventional built environment data such as POI, street view images not only contain POIs information but also supply abundant scene information, such as lights and trees. Besides, street view images record the urban landscape in a detailed and systematic way from the perspective of pedestrians. The scene information is an important environmental condition for criminals to decide whether to commit a crime or not. Therefore, street view images have more advantages to study criminal activities compared with traditional data. Now, a few studies began to explore the correlation between streetscape features and criminal activities [2, 19]. For instance, the associations between different streetscape visual features and violent crimes were explored using Google Street View(GSV) images to find out the key streetscape elements that affect criminal behaviors [2, 19]. Moreover, the complex relationship between criminal behaviors and streetscape features extracted from GSV was studied by combining with social economy, environmental context, and other crime prediction information [33, 49].

Despite the above contributions, there still exist following drawbacks: firstly, using the manual audit method to extract street physical elements from GSV has the disadvantages of low efficiency, strong subjectivity and difficult to implement on a large scale. Hence, it is necessary to combine intelligent technology with GSV to automatically quantify the streetscape features on a large scale. Secondly, the existing studies mostly analyzed the relationship between built environment and crimes on a global scale, ignoring the influences variation of streetscape characteristics in different regions, and failing to recognize the key streetscape factors that affect different types of crime. This makes the deep impact mechanism of the street environment on criminal behavior still unclear.

5 Conclusions

Taking uptown and downtown Manhattan as study areas, this study automatically measured the streetscape features quantitatively using deep learning technology from street-level GSV firstly. Then, poisson regression models are conducted to explore the correlation between the streetscape factors and criminal activities to find the main streetscape elements that affect criminal behaviors from a global perspective. Finally, GWPR models are used to further study the influence intensity between eight streetscape factors and criminal activities as well as their spatially varying and difference, and to find out the key streetscape elements that influence criminal behaviors from a local perspective. The main findings are as follows:

- 1) The correlation between the streetscape factors and crimes in downtown is stronger than that in uptown based on the global poisson regression results.
- 2) MI has a positive correlation with criminal activities and PSI has a negative correlation with criminal activities through the global regression analysis. The influence of SVI and NAI on crime is relatively gentle.
- 3) The five visual factors of PSI, GVI, BVI, LVI and MI have a significant spatial influence on criminal activities based on the GWPR regression results. Especially, the influence intensity of different streetscape elements on crime is significantly different at street level, and the streetscape elements that influence specific criminal activities in each street can be identified according to the GWPR results.
- 4) The influence of streetscape elements on criminal activities is also influenced by the socio-economic, cultural and other factors in the regional crime occurred, and this influence plays a decisive role in the occurrence of crime in certain situations. For example, the influence of GVI on criminal activities is opposite in different regions, and the relationship between LVI and criminal activities shows greatly spatial heterogeneity. This can be explained as the impact of socio-economic and other factors. Therefore, in the practice of crime prevention through street design, it is necessary to take the local streetscape factors and regional socioeconomic level into account.

This study still has limitations and leaves room for future explorations. The first concern is the time consistency of google street view images [46], which is a difficult but inevitable problem. Street view images were not all taken during the same period, some of them were taken during winter

or summer, and some were taken during holidays or work-days. This article only uses visual inspection to exclude images that are not in the same period or problematic, which has certain limitations. Then, the influence of the interaction of different visual factors and the combination of different indicators on crime needs to be further explored. In the future, we will study the spatial pattern changes of criminal activities and the impact of street physical environment factors on different spatial scales by integrating multi-source data(such as built environment survey data, geotagged social media data, socio-economic data, etc.).

Acknowledgements The work was supported by the National Natural Science Foundation of China (No. 61872050), the Chongqing Basic and Frontier Research Program (No. cstc2018jcyjAX0551), the Fundamental Research Funds for the Central Universities (No.2018CDJSK03XK01), and the Chongqing Technology Innovation and Application Development Key Project (No. ctsc2019jscx-gksbX0066) . Wei Yang and Chao Chen are the corresponding authors for this paper.

References

- Troy A, Nunery A, Grove J M. The relationship between residential yard management and neighborhood crime: an analysis from baltimore city and county. *Landscape and Urban Planning*, 2016, 147: 78-87
- He L, Páez A, Liu D. Built environment and violent crime: an environmental audit approach using google street view. *Computers, Environment and Urban Systems*, 2017, 66: 83-95
- Wang L, Lee G, Williams I. The spatial and social patterning of property and violent crime in toronto neighbourhoods: a spatial-quantitative approach. *ISPRS International Journal of Geo-Information*, 2019, 8(1): 51
- Cozens P, Davies T. Crime and residential security shutters in an Australian suburb: exploring perceptions of 'eyes on the street', social interaction and personal safety. *Crime Prevention and Community Safety*, 2013, 15(3): 175-191
- Reynald D M, Elffers H. The future of newman's defensible space theory: linking defensible space and the routine activities of place. *European Journal of Criminology*, 2009, 6(1): 25-46
- Wilson J Q, Kelling G L. Broken windows. *Atlantic Monthly*, 1982, 249(3): 29-38
- Michael Cozens P, Saville G, Hillier D. Crime prevention through environmental design (cpted): a review and modern bibliography. *Property management*, 2005, 23(5): 328-356
- Cozens P, Love T. A review and current status of crime prevention through environmental design (cpted). *Journal of Planning Literature*, 2015, 30(4): 393-412
- Chalfin A, Hansen B, Lerner J, Parker L. Reducing crime through environmental design: evidence from a randomized experiment of street lighting in new york city. *National Bureau of Economic Research*, 2019
- Lee I, Jung S, Lee J, Macdonald E. Street crime prediction model based on the physical characteristics of a streetscape: analysis of streets in low-rise housing areas in South Korea. *Environment and Planning B: Urban Analytics and City Science*, 2019, 46(5): 862-879
- Barnum J D, Caplan J M, Kennedy L W, Piza L E. The crime kaleidoscope: a cross-jurisdictional analysis of place features and crime in three urban environments. *Applied Geography*, 2017, 79: 203-211
- Wolfe M K, Mennis J. Does vegetation encourage or suppress urban crime? evidence from Philadelphia, PA. *Landscape and Urban Planning*, 2012, 108(2-4): 112-122
- Zhou H, Liu L, Lan M, Yang B, Wang Z. Assessing the impact of nightlight gradients on street robbery and burglary in Cincinnati of Ohio state, USA. *Remote Sensing*, 2019, 11(17): 1958
- Patino J E, Duque J C, Pardo-Pascual J E, Ruiz L A. Using remote sensing to assess the relationship between crime and the urban layout. *Applied Geography*, 2014, 55: 48-60
- Rundle A G, Bader M D M, Richards C A, Neckerman K M, Teitler J O. Using google street view to audit neighborhood environments. *American Journal of Preventive Medicine*, 2011, 40(1): 94-100
- Andersson V O, Birck M A F, Araujo R M. Investigating crime rate prediction using street-level images and siamese convolutional neural networks. In: *Proceedings of Latin American Workshop on Computational Neuroscience*. 2017: 81-93
- Fu K, Chen Z, Lu C. Streetnet: preference learning with convolutional neural network on urban crime perception. In: *Proceedings of the 26th ACM SIGSPATIAL International Conference on Advances in Geographic Information Systems*. 2018: 269-278
- Chen L C, Zhu Y, Papandreou G, Schroff F, Adam H. Encoder-decoder with atrous separable convolution for semantic image segmentation. In: *Proceedings of the European Conference on Computer Vision (ECCV)*. 2018: 801-818
- Li X, Zhang C, Li W. Does the visibility of greenery increase perceived safety in urban areas? evidence from the place pulse 1.0 dataset. *ISPRS International Journal of Geo-Information*, 2015, 4(3): 1166-1183
- Li X, Ratti C, Seiferling I. Quantifying the shade provision of street trees in urban landscape: a case study in Boston, USA, using google street view. *Landscape and Urban Planning*, 2018, 169: 81-91
- Li X, Zhang C, Li W, Ricard R, Meng Q, Zhang W. Assessing street-level urban greenery using google street view and a modified green view index. *Urban Forestry and Urban Greening*, 2015, 14(3): 675-685
- Dai Z, Hua C. The improvement of street space quality measurement method based on streetscape. *Planners*, 2019, 35(9): 57-63
- Tang J, Long Y. Metropolitan street space quality evaluation: second and third ring of beijing, inner ring of shanghai. *Planners*, 2017, 33(2): 68-73
- Yue H, Zhu X, Ye X, Hu T, Kudva S. Modelling the effects of street permeability on burglary in Wuhan, China. *Applied Geography*, 2018, 98: 177-183
- Tobler W R. A computer movie simulating urban growth in the Detroit region. *Economic Geography*, 1970, 46(sup1): 234-240
- Fuentes C M, Jurado V. Spatial pattern of motor vehicle thefts in Ciud-

- dad Juárez, Mexico: an analysis using geographically weighted poisson regression. *Applied Geography*, 2019, 5(1-2): 176-191
27. Bidanset P E, Lombard J R. Evaluating spatial model accuracy in mass real estate appraisal: a comparison of geographically weighted regression and the spatial lag model. *Cityscape*, 2014, 16(3): 169-182
 28. Getis A. A history of the concept of spatial autocorrelation: a geographer's perspective. *Geographical Analysis*, 2008, 40(3): 297-309
 29. Cotte Poveda A. Violence and economic development in Colombian cities: a dynamic panel data analysis. *Journal of International Development*, 2012, 24(7): 809-827
 30. Ekkel E D, de Vries S. Nearby green space and human health: evaluating accessibility metrics. *Landscape and Urban Planning*, 2017, 157: 214-220
 31. Cabrera-Barona P F, Jimenez G, Melo P. Types of crime, poverty, population density and presence of police in the metropolitan district of Quito. *ISPRS International Journal of Geo-Information*, 2019, 8(12): 558
 32. Fuentes C M, Hernandez V. Housing finance reform in Mexico: the impact of housing vacancy on property crime. *International Journal of Housing Policy*, 2014, 14(4): 368-388
 33. Xu C, Liu L, Zhou S, Jiang C. Spatial heterogeneity of micro-spatial factors' effects on street robberies: a case study of DP peninsula. *Geographical Research*, 2017, 36(12): 2492-2504
 34. Wang H, Kifer D, Graif C, Li Z. Crime rate inference with big data. In: *Proceedings of the 22nd ACM SIGKDD International Conference on Knowledge Discovery and Data Mining*. 2016: 635-644
 35. Kadar C, Pletikosa I. Mining large-scale human mobility data for long-term crime prediction. *EPJ Data Science*, 2018, 7(1): 26
 36. Setiawan I, Dede M, Sugandi D, Widiawaty M A. Investigating urban crime pattern and accessibility using geographic information system in Bandung City. *KnE Social Sciences*, 2019: 535-548
 37. Steinbach R, Perkins C, Tompson L, Johnson S, Armstrong B, Green J, Grundy C, Wilkinson P, Edwards P. The effect of reduced street lighting on road casualties and crime in England and Wales: controlled interrupted time series analysis. *Journal of Epidemiol and Community Health*, 2015, 69(11): 1118-1124
 38. Ye C, Chen Y, Li J. Investigating the influences of tree coverage and road density on property crime. *ISPRS International Journal of Geo-Information*, 2018, 7(3): 101
 39. Davies T, Johnson S D. Examining the relationship between road structure and burglary risk via quantitative network analysis. *Journal of Quantitative Criminology*, 2015, 31(3): 481-507
 40. Wang J, Wu N, Lu X, Zhao X, Feng K. Deep trajectory recovery with fine-grained calibration using kalman filter. *IEEE Transactions on Knowledge and Data Engineering*, 2019
 41. Chen C, Jiao S, Zhang S, Liu W, Feng L, Wang Y. TripImputor: real-time imputing taxi trip purpose leveraging multi-sourced urban data. *IEEE Transactions on Intelligent Transportation Systems*, 2018, 19(10): 3292-3304
 42. Chen C, Ding Y, Xie X, Zhang S, Wang Z, Feng L. TrajCompressor: an online map-matching-based trajectory compression framework leveraging vehicle heading direction and change. *IEEE Transactions on Intelligent Transportation Systems*, 2019, 21(5): 2012-2028
 43. Chen C, Zhang D, Guo B, Ma X, Pan G, Wu Z. TripPlanner: personalized trip planning leveraging heterogeneous crowdsourced digital footprints. *IEEE Transactions on Intelligent Transportation Systems*, 2014, 16(3): 1259-1273
 44. Chen C, Zhang D, Ma X, Guo B, Wang L, Wang Y, Sha E. CrowdDelivery: planning city-wide package delivery paths leveraging the crowd of taxis. *IEEE Transactions on Intelligent Transportation Systems*, 2016, 18(6): 1478-1496
 45. Wang J, Wu J, Wang Z, Gao F, Xiong Z. Understanding urban dynamics via context-aware tensor factorization with neighboring regularization. *IEEE Transactions on Knowledge and Data Engineering*, 2019
 46. Wang J, Wang Y, Zhang D, Lv Q, Chen C. Crowd-powered sensing and actuation in smart cities: current issues and future directions. *IEEE Wireless Communications*, 2019, 26(2): 86-92
 47. Gao J, He Y, Wang Y, Wang X, Wang J, Peng G, Chu X. STAR: spatio-temporal taxonomy-aware tag recommendation for citizen complaints. In: *Proceedings of the 28th ACM International Conference on Information and Knowledge Management*. 2019: 1903-1912
 48. Gong F, Zeng Z, Zhang F, Li X, Ng E, Norford L K. Mapping sky, tree, and building view factors of street canyons in a high-density urban environment. *Building and Environment*, 2018, 134: 155-167
 49. Kang H W, Kang H B. Prediction of crime occurrence from multimodal data using deep learning. *PloS one*, 2017, 12(4): e0176244.

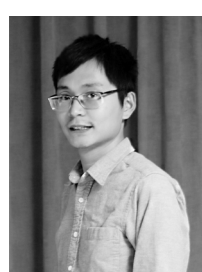


Mingyu Deng is currently a master student at College of Computer Science, Chongqing University, Chongqing, China.

She obtained her bachelor degree of Computer Science and Technology of Chongqing University of Posts and Telecommunications in 2018. Her research interests include smart cities and data visualization.



Wei Yang received the PhD degree in School of Resource and Environmental Science at Wuhan University, China in 2019. He is currently a Lecturer at Chongqing University, Chongqing, China. His research interests include trajectory data mining, human behavior analysis, GIS and smart city.



Chao Chen is a full professor at College of Computer Science, Chongqing University, Chongqing, China. He obtained his Ph.D. degree from Pierre and Marie Curie University and Insti-

tut Mines-Télécom/Télécom SudParis, France in 2014. He received the B.Sc. and M.Sc. degrees in control science and control engineering from Northwestern Polytechnical University, Xi'an, China, in 2007 and 2010, respectively. Dr. Chen got published over 80 papers including 20 ACM/IEEE Transactions. His work on taxi trajectory data mining was featured by IEEE Spectrum in 2011 and 2016 respectively. He was also the recipient of the Best Paper Runner-Up Award at MobiQuitous 2011.

In 2009, he worked as a Research Assistant with Hong Kong Polytechnic University, Kowloon, Hong Kong. His research interests include pervasive computing, mobile computing, urban logistics,

tics, data mining from large-scale GPS trajectory data, and big data analytics for smart cities.



Chenxi Liu is currently a master degree candidate at College of Computer Science, Chongqing University. He received his bachelor degree from the School of Optical and Electronic Information of Huazhong University of Science and Technology in 2017. His research interests include reinforcement learning and ride-sharing platform optimization.